MONTE CARLO SIMULATIONS OF THE 2+1 DIMENSIONAL FOKKER-PLANCK EQUATION: SPHERICAL STAR CLUSTERS CONTAINING MASSIVE, CENTRAL BLACK HOLES

Stuart L. Shapiro
Cornell University
Center for Radiophysics and Space Research
Space Sciences Building
Ithaca, New York 14853

ABSTRACT. The dynamical behavior of a relaxed star cluster containing a massive, central black hole poses a challenging problem for the theorist and intriguing possibilities for the observer. The historical development of the subject is sketched and the salient features of the physical solution and its observational consequences are summarized.

The full dynamical problem of a relaxed, self-gravitating, large N-body system containing a massive central black hole has all the necessary ingredients to excite the most dispassionate many-body, computational physicist: it is a time-dependent, multidimensional, nonlinear problem which must be solved over widely disparate length and time scales simultaneously. The problem has been tackled at various levels of approximation over the years. A new 2+1 dimensional Monte Carlo simulation code has been developed in appreciable generality to solve the time-dependent Fokker-Planck equation in E-J space for this problem. The code incorporates such features as (1) a particle "cloning and renormalization" scheme to provide a statistically reliable population of test particles in low density regions of phase space and (2) a time-step "adjustment" algorithm to ensure integration on local relaxation timescales without having to follow typical particles on orbital trajectories. However, critical regions in phase space (e.g. disruption "loss-cone" trajectories) can still be followed on orbital timescales. Numerical results obtained with this Monte Carlo scheme for the dynamical structure and evolution of globular star clusters and dense galactic nuclei containing massive black holes are reviewed.

Recent dynamical integrations of the Einstein field equations for spherical, collisionless (Vlasov) systems in General Relativity suggest a possible origin for the supermassive black holes believed to power quasars and active galactic nuclei. This scenario is discussed briefly.

I. INTRODUCTION

Several years ago we embarked on a major program at Cornell to set up
and solve on the computer the Fokker-Planck equation in 2+1 dimensional
phase space. The purpose of this exploration was to study the struc-
ture and evolution of large N-body, self-gravitating, spherical stellar
systems, like globular clusters and dense galactic nuclei. We were
particularly intrigued by the possibility of massive central black
holes residing in such systems and this aspect of the problem served as
a focus for much of our work.

As it has developed, the study of the Fokker-Planck equation has
become just one, albeit essential, component of a much broader effort
at Cornell in large-scale computational astrophysics and relativity.
Our current emphasis is on solving the general Boltzmann equation,

$$\frac{Df}{Dt} = \left(\frac{\partial f}{\partial t}\right)_{coll} , \tag{1}$$

in many different physical regimes where gravity provides the dominant
long-range interaction.

Our motivation for tackling the Boltzmann equation is both
physical and computational. Physically, this equation encompasses a
huge range of interesting, many-body phenomena. Computationally, the
Boltzmann equation provides a nontrivial, multidimensional arena to
explore nonlinear dynamics on the computer. We shall elaborate on
these points below with reference to the specific star cluster problem
that is the subject of this review.

Some of our recent computational work revolving around eqn. (1) is
summarized in Table 1. This table is a vivid illustration of the fact
that an enormous and diverse range of gravitation physics is embodied
in eqn. (1). This review will focus on the Fokker-Planck regime of
eqn. (1). In this limit, the relaxation timescale of the system under
investigation, t_r, greatly exceeds the dynamical or crossing timescale,
t_d, but is shorter than characteristic integration timescale of inter-
est, t. In stellar dynamics, t is usually the age of the stellar sys-
tem and, typically, t ~ H^{-1} ~ 10^{10} yrs, where H is Hubble's constant.
We will, however, also provide a "sneak preview" of some recent
advances we have made in solving the collisionless Boltzmann (i.e.
Vlasov) equation for spherical systems in full General Relativity.
For such cases we set the collision terms $(\partial f/\partial t)_{coll}$ equal to zero in
eqn. (1).

As we shall shortly describe, it is the Fokker-Planck regime which
is relevant to addressing the question, "What is the dynamical influ-
ence of a massive black hole in a relaxed stellar system?". However,
we shall point out later that the relativistic Vlasov regime, may,
following the Fokker-Planck epoch, hold the clue to answering the
question, "What is the origin of the supermassive black holes believed
to reside in quasars and active galactic nuclei (AGNs)?".

Most of the large-scale numerical work at Cornell is currently
performed on Floating Point Systems (FPS) 190L or 164 Array Processors,

hosted by an IBM 3081 mainframe computer. ⌈For a discussion of the merits of this machine, and an overview of some of the computational work summarized in Table 1 and performed on these processors see Farouki, Shapiro and Teukolsky (1983). For a discussion of the more recent work on the Vlasov equation in General Relativity, see Shapiro and Teukolsky (1985 a,b,c).

TABLE 1

CORNELL BOLTZMANN EQUATION COMPUTATIONS

REGIME:	Vlasov (Collisionless)		Fokker−Planck (Secularly Collisional)	Fluid (Collision-Dominated)	
TIME-SCALE ORDERING:	$t_r \gg t \gg t_d$		$t \gg t_r \gg t_d$	$t \gg t_d \gg t_r$	
APPLICATIONS:	Galaxy and Galaxy Cluster Dynamics		Globular Cluster and Dense Galactic Nuclei Dynamics	Hydrodynamics	
GRAVITY	Newtonian	General Relativity	Newtonian	Newtonian	General Relativity
SPATIAL SYMMETRY	Arbitrary	Spherical	Spherical	Axisymmetric	Spherical
COMPUTATIONAL DIMENSIONS	$2K+1$ $(K=3)$	$2K+1$ $(K=1)$	$2K+1$ $(K=1)$	$K+1$ $(K=2)$	$K+1$ $(K=1)$
GOVERNING NONLINEAR EQUATIONS	ODE's	ODE's + PDE's	PDE's	PDE's	PDE's
TECHNIQUE	Particle Simulations	Particle Simulations + Finite Differencing	Monte Carlo Particle Simulations	Finite Differencing	Finite Differencing

II.   3-FOLD MOTIVATION FOR TACKLING THE PROBLEM

Studying the dynamical structure and evolution of a relaxed stellar
system (e.g. a globular cluster or dense galactic nucleus) containing a
massive black hole is a pursuit with a 3-fold motivation, as we shall
now discuss.

a)   Theoretical Motivation

The formation of a supermassive black hole is one of at least two
plausible outcomes of stellar core collapse. Both possibilities were
enumerated by Spitzer (1975) almost a decade ago.
     In the "point-mass scenario", homological core collapse (i.e. the
'gravothermal catastrophe') terminates with the formation of hard
binaries near the cluster center. Further gravitational encounters
between these binaries and neighboring single stars and binaries cause
the binaries to become more tightly bound at the expense of the ambient
core. In fact, some stars may be ejected from the core altogether by
this binary "heating" mechanism. This scenario has been the focus of
considerable attention of late; it is the subject of most of the
theoretical papers in this volume.
     In the alternative "finite-size star scenario", core collapse
ultimately leads to star collisions and coalescence in the core and to
the run-away build up of one (or more) supermassive star. This short-
lived supermassive star ultimately collapses to form a supermassive
black hole at the cluster center. Not surprisingly, the details of the
all-important collision-coalescence phase of this scenario are subtle
and yet to be fully resolved. [See Lightman and Shapiro (1978) for a
discussion and references.] However, as we shall discuss below, given
the presence of a massive, central black hole, the dynamical fate of
the cluster which evolves under its influence has been worked out, at
least for suitably approximate circumstances. So for at least one of
the two theoretical scenarios - that involving a supermassive black
hole - the answer to the question, "What lies beyond core collapse?"
can be concretely answered.

b)   Observational Motivation

The presence of a supermassive black hole has been invoked often to
explain diverse forms of 'anomalous' activity observed at the centers
of various stellar systems. Table 2 offers a glimpse of this trend.

c)   Computational Motivation

A massive black hole in a relaxed star cluster provides a unique cosmic
setting in which to solve the 2+1-dimensional Fokker-Planck equation.
The problem is highly nonlinear, multidimensional and is characterized
by widely varying length scales. These attributes are particularly
appealing to a computational physicist. Thus, for all its deceptive
simplicity ("merely" Newton's laws of motion in a weak gravitational
field for N point-masses), the problem of a massive black hole in a

relaxed stellar system poses an exciting and difficult computational challenge.

In recent years, "computational field theory on a space-time lattice" has become a booming enterprise. This activity is pursued by many-body theorists in several branches of physics, including solid-state, particle, plasma, astrophysics and relativity. The Fokker-Planck problem discussed in this paper falls into this broad category of computational problems: the 'field' here is Newtonian gravity and the 'space' is E-J phase space.

Progress achieved in solving a nonlinear problem in physics often transcends the specific discipline in which the problem was originally formulated and the specific application initially under investigation. It was with this notion in mind that the Cornell group initiated its study of the massive black hole problem.

TABLE 2   OBSERVATIONAL BASIS FOR SUPERMASSIVE BLACK HOLES IN STELLAR SYSTEMS

Phenomenon	Examples	References
optical light 'cusps'	NGC 6624, 6681 and 7078 (M15) M87	Djorgovski and King (1984), Young et al. 1978
star count 'excesses'	NGC 1851	Bahcall et al. (1977)
velocity dispersion rise	M87	Sargent et al. (1978)
X-ray sources	X-ray globular clusters; AGNs and quasars	Grindlay (1977); Gursky and Schwartz (1977)
broad emission lines and rapid time variability	AGNs and quasars; (e.g. NGC 4151)	Strittmatter and Williams (1976); Ulrich et al. (1984)
energetic activity: high lumi-nosities and jets	AGNs and quasars	Rees (1984)

III.   HISTORY OF THE PROBLEM

Given the many motivating factors outlined in the previous section for
considering the influence of a massive black hole in a star cluster, it
is not surprising that an enormous amount of work has been done on this
problem by a very large number of researchers over the years. Indeed,
virtually every dynamicist has thought about this issue at one time or
another and a good many have published on the subject!
      With this in mind, it is amusing to trace the historical develop-
ment of the topic. A light-hearted version of such a review is given
in Box 1. Please note that this capsule summary of some of the high-
lights in the formulation and analysis of the problem is both highly
personalized and very incomplete. Other authors may rightfully have an
entirely different perspective on the development of the problem. It
is also hoped the reader will excuse this author for dramatizing the
Cornell group's contributions during this brief stroll down Memory
Lane. They are mentioned mainly to show the extent of the group's
interest and involvement in the subject and not to attach undue
significance to our work.

IV.   FORMULATION OF THE IDEALIZED PROBLEM

In its simplest version, the problem focuses on the steady-state
distribution and tidal disruption rate of bound stars near a central
black hole M embedded in a static cluster. In this version, one makes
the following basic assumptions (Bahcall and Wolf 1976; Lightman and
Shapiro 1977):

      1. A massive hole, M, is situated at the center of a spherical
cluster containing a very large number, N, of stars in the core.
      2. All stars have equal mass m $\ll$ M and radius r.
      3. The mass, M, is significantly less than the mass of the
cluster core but much larger than the total mass of (bound) stars
inside the accretion or 'cusp' radius r_a, where

$$r_a ~ \sim ~ \frac{GM}{\langle v^2 \rangle} ~ \sim ~ 4 \times 10^{-2} \text{ pc} \left(\frac{\langle v^2 \rangle}{100 \text{ km}^2/\text{s}^2} \right)^{-1} M_3 \quad , \qquad (2)$$

Here $\langle v^2 \rangle$ is the mean squared velocity dispersion in the core and
$M_3 \equiv M/10^3 M_\odot$.
      4. Conditions in the central core of the cluster remain constant
in time, so that a steady-state can be achieved near the black hole.
The ambient (unbound) core stars far outside r_a satisfy an isothermal
distribution.
      5. A star is tidally disrupted and removed whenever it passes
within a distance r_D of M, where

```
┌─────────────────────────────────────────────────────────────┐
│                          Box 1                                │
│                                                               │
│            THE DYNAMICAL ANALYSIS OF MASSIVE                  │
│            BLACK HOLES IN STAR CLUSTERS :                     │
│                                                               │
│               SOME "GOLDEN MOMENTS"                           │
```

AUTHOR (S)	CONTRIBUTION (S)	REMARKS
EINSTEIN (1939)	Shows impossibility of 'Schwarzschild singularities' in static spherically symmetric collisionless clusters of circularly orbiting particles	Relativistic stellar dynamics is born !
ZEL'DOVICH and PODURETS (1965) IPSER (1969) FACKERELL , IPSER and THORNE (1969)	Suggest how 'gravothermal catastrophe' and collisions might drive a cluster relativistically unstable, leading to catastrophic collapse and supermassive BH formation	Clusters of little BH's can produce a big BH
SPITZER (1971 , 1975) LYNDEN-BELL (1967, 1969) COLGATE (1967) SANDERS (1970)	Suggest, alternatively, how 'gravothermal catastrophe' might drive star collisions and coalescence, leading to buildup of supermassive stars and possibly, super-massive BH's	Analysis of late core collapse forces abandon-ment of point-mass approx.
WYLLER (1970) WOLFE and BURBIDGE (1970) TRURAN and CAMERON (1972)	Suggest that a supermassive BH in a star cluster might be uncovered by enhanced star density around it	The stage is set!
PEEBLES (1972) (a, b)	Insightful formulation of BH in glob cluster problem : (1) delineates role of tidal disruption of stars by BH- inward $\mathscr{F}$, outward $\mathscr{E}$ (2) suggests possibility of observable light 'cusps' (3) suggests nonthermal power-law 'cusp' distribution function : $$f(E) \propto |E|^p$$ $$\Rightarrow n(r) \propto r^{-(p + 3/2)}$$	Argues for $p = 3/4$ whereas $p = 1/4$ is more appropriate

Box 1 (cont.)

AUTHOR(S)	CONTRIBUTION(S)	REMARKS
BAHCALL and OSTRIKER (1975) SILK and ARONS (1975)	Suggest supermassive BH ($M/M_\odot \sim 10^2 - 10^3$) as the source of X-rays in globular clusters	The search is on!
BAHCALL and WOLF (1976, 1977)	Careful 1D FP calculation of $f(E)$ and $n(r)$: $p = 1/4$; formulate detectability criteria; estimate rms radial offset of BH from center	"The cusp unveiled"
ZEL'DOVICH and NOVIKOV (1971) HILLS (1975)	Stellar capture rate by BH's in galaxies is estimated	The BH appetite is assessed
FRANK and REES (1976) LIGHTMAN and SHAPIRO (1976 a,b)	Stellar capture rate by BH's in glob clusters is estimated; approximate 2D FP determination of $f(E,J)$, $n(r)$, $\mathcal{F}$ and $\mathcal{E}$, including scaling	
SHAPIRO (1977)	Homological model for time-dependent evolution of cluster with BH : core collapse halted and reversed ; eventual cluster dissolution in Galactic tidal field.	'Born again' clusters
MARCHANT and SHAPIRO (1978) COHN and KULSRUD (1978)	Careful 2D FP calculation of $f(E,J)$, $n(r)$ $\mathcal{F}$ and $\mathcal{E}$	Back-of-envelopes replaced by large-scale computations
GRINDLAY (1981,1983) GRINDLAY et. al. (1984)	Precise (1") positions of 8 cluster X-ray sources are measured by the Einstein Observatory : their radial offset argues against massive ($M/M_\odot \geq 3$) BH's	"The saddest words of Mice and Men..."
LIGHTMAN, PRESS and ODENWALD (1978) FALL and MALKAN (1978) LIGHTMAN (1982) COHN and HUT (1984)	Preliminary analysis of cluster data for post-collapse behavior	Dynamical model builders take note!

```
┌─────────────────────────────────────────────────────────────┐
│                      Box 1 (cont.)                          │
│                                                              │
│  ─────────────────────────────────────────────────────────  │
│    AUTHOR(S)              CONTRIBUTION(S)         REMARKS     │
│                                                              │
│  ZEL'DOVICH and NOVIKOV (1971)   Application of theory to    │
│                                  dense galactic nuclei:  "BH's are │
│  HILLS (1975)                    models for quasars and  where you │
│  REES (1977, 1978)               AGN's                   find them" │
│  YOUNG, SHIELDS and WHEELER(1977)                        (Peebles 1972a) │
│  FRANK (1978)                                                │
│  McMILLAN, LIGHTMAN and                                      │
│     COHN (1982)                                              │
│  DUNCAN and SHAPIRO (1983)                                   │
│  ─────────────────────────────────────────────────────────  │
│                                                              │
│                                                              │
│        Other Contributors:  Caveats and Controversies        │
│                                                              │
│                                                              │
│    see, e.g.,  IPSER (1978)                                  │
│                BISNOVATYI — KOGAN, CHURAYEV and KOLOSOV (1982)│
│                DOKUCHAYEV and OZERNOI (1977)                 │
│                LIN and TREMAINE (1980)                       │
│                NORMAN and SILK (1982)                        │
│                                                              │
└─────────────────────────────────────────────────────────────┘
```

$$r_D \sim r\,(M/m)^{1/3} \sim 2 \times 10 \text{ pc} \left(\frac{r}{R_\odot}\right)\left(\frac{m}{M_\odot}\right)^{-1/3} M_3^{1/3} , \qquad (3)$$

Immediate consequences of the assumption of large N are the following familiar results:

1a. Only a negligible fraction of the stars in the cluster are in binary systems (Spitzer and Hart 1971).

1b. The predominant relaxation process between stars is via repeated, two-body, small-angle scattering in the hole's r^{-1} "Coulomb" potential.

1c. The dynamical timescale t_d is significantly shorter than the relaxation timescale t_r everywhere. Thus, by Jean's Theorem, the distribution function depends only on E (energy) and J (magnitude of angular momentum): $f = f(E,J)$.

The goal, then, is to calculate $f(E,J)$. Given $f(E,J)$ we can then determine the steady-state density profile $n(r)$ and rms velocity profile $v_{rms}(r)$ of bound stars in the cusp. In addition, we want to determine the rate of tidal disruption of stars by the hole, F, which

in steady-state is precisely equal to the net inward drift rate of
stars from the isothermal core into the cusp. Finally, we need to
determine the corresponding cluster heating rate, $\dot{E}$, due to the de-
struction of bound stars at r_D by the hole.

V. APPROXIMATE SOLUTION OF THE IDEALIZED PROBLEM

a) Simple Scaling Argument

Following Shapiro and Lightman (1976) we present here a simple scaling
argument for the form of the stellar distribution inside the cusp. The
derivation focuses on bound stars well inside r_a but far outside r_D.
As Peebles (1972 a,b) originally pointed out, these stars cannot main-
tain thermal equilibrium with the ambient core stars, due to disruption
at r_D. On the other hand, stars deep in the cusp but far outside r_D
should presumably be moving nearly isotropically, so it is reasonable
to look for a scale-free, isotropic, power-law distribution function of
the form

$$f(E) \propto |E|^p \quad . \tag{4}$$

Now from eqn. (4) and the assumptions listed in Section IV it immedi-
ately follows that the mean energy per unit mass of star at r is given
by

$$E \sim - GM/r \quad , \tag{5}$$

the stellar velocity dispersion is given by

$$\langle v^2 \rangle \sim GM/r \quad , \tag{6}$$

and the stellar density profile is given by

$$n(r) \propto r^{-(p + 3/2)} \quad , \tag{7}$$

so the problem of determining the stellar distribution reduces to
finding p.
    Focus, then, on stars in a typical spherical shell between r and
2r in the cusp. The net inward flux of stars is then

$$F \sim \frac{n(r)\, r^3}{t_F(r)} = \text{constant, independent of r} \quad , \tag{8}$$

where t_F is the net diffusion timescale for inward star transport in
the cusp. The net outward flux of energy is

$$E \sim \frac{n(r) \; r^3 \; E}{t_E(r)} = \text{constant, independent of } r \quad , \qquad (9)$$

where t_E is the net diffusion timescale for outward energy transport. In steady-state F and E are constant, independent of radius. Now eqns. (8) and (9) immediately relate t_E and t_F:

$$t_E \propto t_F \; r^{-1} \; . \qquad (10)$$

Thus t_E is shorter than t_F because for each star moving <u>inward</u> from $2r$ to r there is almost simultaneously a corresponding star <u>moving outward</u> from r to $2r$, so that the <u>net</u> star flux is small. However, at $\overline{r_D \text{ there}}$ are no outgoing stars so <u>the</u> net diffusion timescales for star and energy transport are comparable there. This fact determines the proportionality constant in eqn. (2):

$$t_E(r) \sim (r_D/r) \; t_F(r) \qquad (11)$$

Now no quantity can be transported in a relaxed cluster on a timescale shorter than the local relaxation timescale,

$$t_r \sim \frac{\langle v^2 \rangle^{3/2}}{G^2 m^2 n^2} \quad . \qquad (12)$$

So setting $t_E(r)$ ($< t_F(r)$ for $r > r_D$) equal to t_r everywhere and using eqns. (5), (6) and (12) in eqn. (9) yields

$$n(r) \propto r^{-7/4} \; , \qquad r_a \gg r \gg r_D \qquad (13)$$

or, from eqn. (6),

$$p = 1/4 \quad . \qquad (14)$$

This result was first derived by Bahcall and Wolf (1976) (hereafter BW) from a detailed integration of the 1-dimensional Fokker-Planck equation for $f(E)$. The density profile in a cluster containing a black hole is shown schematically in Fig. 1.

b) Some Immediate Observational Consequences

(1) <u>Black Hole Mass Limits</u>. Upon deriving the bound star distribution function, BW showed how it could be applied observationally to set an upper limit to the mass of any central black hole in a star cluster. To detect a massive black hole it is necessary to resolve the cusp region $r \lesssim r_a$. If the cluster is located at distance d from the earth, with the cusp subtending an angle θ_a, we have from eqn. (2)
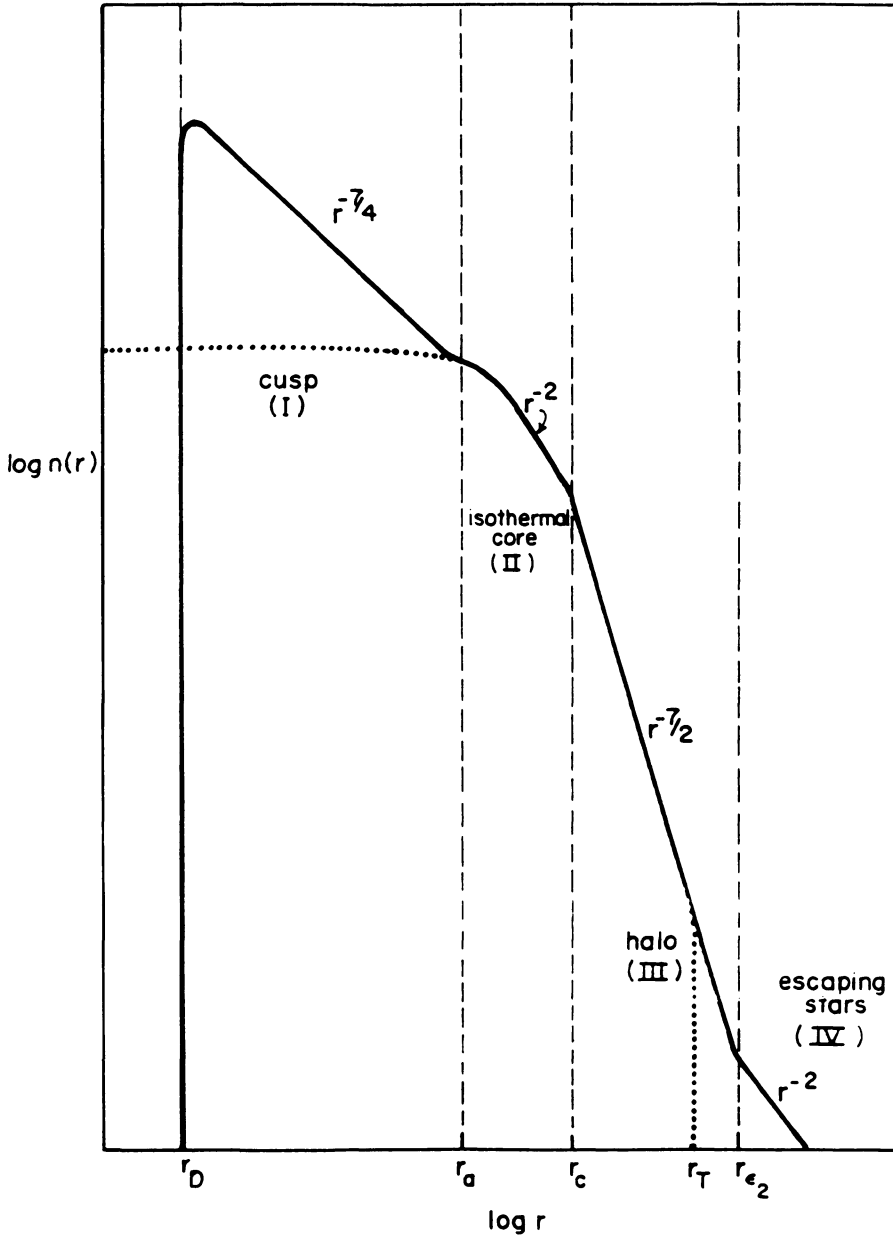
Figure 1: The stellar density n(r) as a function of radius r in an isolated spherical cluster containing a massive, central black hole. In the absence of a black hole, the isothermal core extends from r=0 to the core radius at r=r_c and there is no cusp (dotted line in I). In the presence of the galactic tidal field, the density falls sharply at the galactic tidal radius r_T (dotted line in III). From Shapiro and Lightman (1976).

$$\theta_a ~ \sim ~ 1" ~ \left(\frac{d}{10 \text{ kpc}}\right)^{-1} ~ \left(\frac{\langle v^2 \rangle}{100 \text{ km}^2/\text{s}^2}\right)^{-1} M_3 ~ , \tag{15}$$

which must be compared with the "seeing" disk (i.e. resolution limit) θ_s of an optical telescope:

$\theta_s \sim 1"$ for (optimal) ground based observations,

$\sim 0.1"$ for the Space Telescope . $\tag{16}$

Now the conservative criterion established by BW for believing that a black hole is present in a cluster (i.e. the number of stars within a projected angular radius θ_s from the cluster center is at least F times the unperturbed value for the core, where F ~ 3-10) yields for the minimum detectable black hole mass the value

$$M_{(detectable)} ~ \sim ~ 5 \times 10^3 ~ M_\odot ~ \left(\frac{F}{10}\right)^{4/7} \left(\frac{\theta_c}{5"}\right)^{3/7} \left(\frac{\langle v^2 \rangle}{100 \text{ km}^2/\text{s}^2}\right) \tag{17}$$

where θ_c is the angular radius of the cluster core.

Evidently, ground based observations are only sensitive to black hole masses greater than ~ 5×10^3 $M_\odot$ while future ST observations can detect somewhat smaller masses [see the article by Bahcall in this Proceedings for further discussions of planned ST observations of central cusps in clusters and the associated complications]. Application of eqn. (17) to ground based optical observations of the central density profiles in several X-ray globular clusters indicated central black hole masses (if present) less than ~ 10^4 $M_\odot$. This conclusion is generally consistent with the results of Bahcall et al. (1975) for NGC 7078 (M15), of Bahcall (1976) for NGC 6624 and of Bahcall and Hausman (1976) for NGC 6440 and 6441.

(2) Cusp Profiles. In principle, the observation of an optical light (projected) surface density profile increasing like

$$\sigma \text{ (stars pc}^{-2}) ~ \sim ~ r^{-(p+1/2)} ~ \sim ~ r^{-3/4} \tag{18}$$

toward the center of a relaxed cluster would provide strong evidence for the presence of a central black hole. In practice, however, this observational test is almost impossible to apply. The difficulty stems from the fact that, observationally, it is not easy to distinguish between a black hole induced cusp and, say, an isothermal profile ($\sigma \sim r^{-1}$) predicted by several theories for the post-collapse halo of a cluster [see Inagaki and Lynden-Bell 1983, Heggie 1983, Goodman 1983, and papers in this Proceedings for theoretical discussions of post-collapse clusters without black holes; see Djorgovski and King 1984 and papers by King and Bahcall in this Proceedings for discussions of the observational difficulties].

A more distinguishing characteristic of cusps around black holes is the velocity dispersion profile [eqn. (6)]. The Keplerean rise in $\langle v^2 \rangle$ with decreasing r discriminates between black hole cusps and iso-thermal halos, where $\langle v^2 \rangle$ ~ constant. Unfortunately, velocity profiles are more difficult to measure than light profiles.

(3) <u>Black Hole Cluster Locations</u>. BW and Lightman (1976) showed that in a relaxed cluster core the projected radial offset, R_x, from the core center of a heavy mass M_x satisfies

$$\langle R_x \rangle \sim 0.7 \, r_c \, q^{-1/2} \quad , \quad q \gg 1 \tag{19}$$

where $q = M_x/m$ is the ratio of the heavy mass to the mean stellar mass m in the core and r_c is the core radius. This result has been applied statistically by Grindlay et al. (1984) to eight X-ray globular clusters for which precise (1") positions of the X-ray sources have been measured with the Einstein X-ray Observatory. From the rather large offset of these sources from their cluster centers, the X-ray source masses were determined to be in the range 0.9 - $2M_\odot$. One thus concludes rather definitively that the observed globular cluster X-ray sources are <u>not</u> supermassive black holes [see Grindlay, this volume, for further discussion]. Note that this conclusion by no means rules out the possibility that a massive black hole exists at the centers of these clusters - only that the observed X-ray sources are not massive black holes.

c) The Disruption "Loss-Cone"

Any discussion of the distribution of stars around a black hole which, like the one in Section V.a, presumes an isotropic stellar velocity profile everywhere, f = f(E), cannot be entirely correct. For con-sider, say, those highly eccentric stars which possess sufficiently low J that, at pericenter, they wander inside r_D. These stars are dis-rupted inside r_D and are immediately removed from the system. Clearly, then, the stellar distribution function must depend on J as well as E, as originally emphasized by Frank and Rees (1976) and Lightman and Shapiro (1977).

To appreciate the two-dimensional (anisotropic) character of the problem, consider the distribution of bound stars in velocity space as depicted in Fig. 2. Focus on stars of a given energy E at radius r_E. All stars of energy E move with the same speed $v_E = (GM/r_E)^{1/2}$ at r_E; only the directions of their velocity vectors vary. If their instan-taneous positions in velocity space are marked by the location of the tips of their velocity vectors, then these stars will be found on the surface of a sphere in velocity space, as shown. At this radius stars with maximal angular momentum $J_{max}(E)$ move in a circular orbit about the hole. Stars with critical angular momentum $J_{min}(E)$ just graze the tidal disruption radius r_D at pericenter. As is clear from the figure,
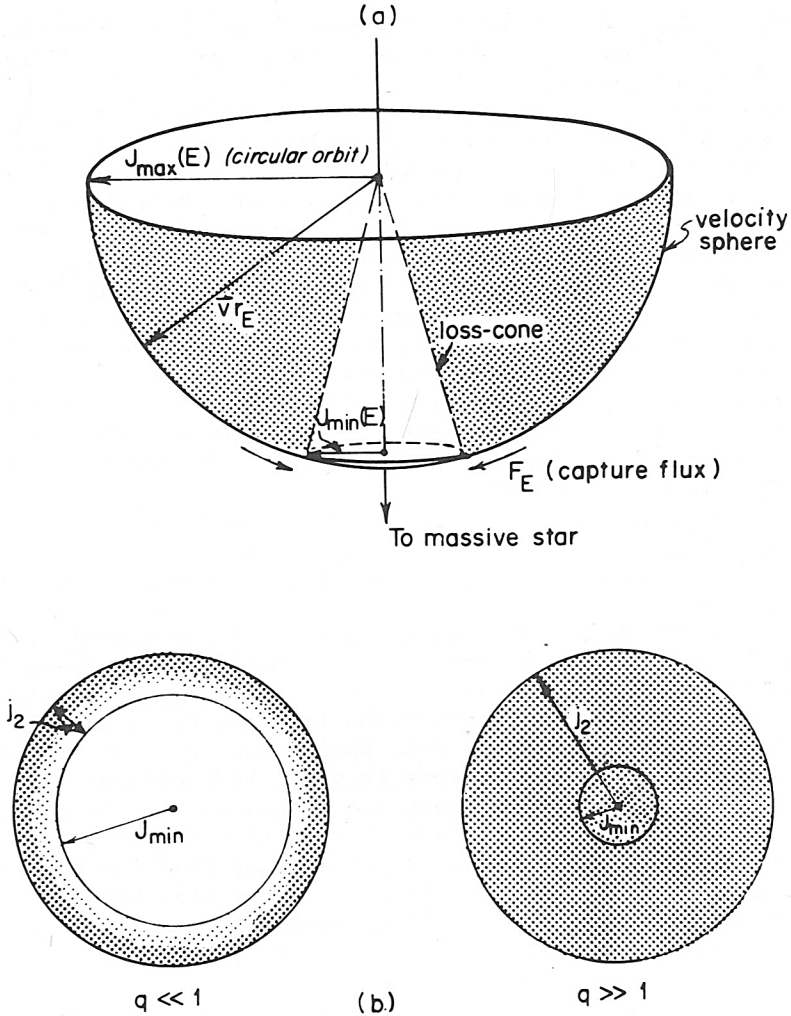
Figure 2: (a) Velocity distribution for ingoing stars with fixed energy E, radius $r_E \equiv GM/2|E|$, and speed $v = (2|E|)^{1/2}$. Stars with angular momentum J in the range $J_{min}(E) \ll J \leq J_{max}(E)$ are distributed nearly uniformly on the velocity sphere, where $J_{min}(E) \equiv [2(E + GM/r_t)]^{1/2} r_t$ and $J_{max}(E) \equiv GM/(2|E|)^{1/2}$. Stars scattered into the loss cone with $J \leq J_{min}(E)$ may be removed from the system in an orbital period. (b) The velocity sphere viewed from below. The quantity j_2 represents the dispersion in ΔJ suffered by a star in one orbital period due to stellar encounters; $q(E) \equiv j_2^2/J_{min}^2(E)$. The phase space density of stars outside the loss cone falls rapidly with J as $J \to J_{min}$ when $q \ll 1$ (the "diffusion" limit), but the density remains nearly uniform when $q \gg 1$ (the "pinhole" limit). In each dynamical time only stars in the ring $J_{min} < J \leq J_{min} + j_2$ may enter the loss cone. From Lightman and Shapiro (1977).

the region $J < J_{min}(E)$ maps out a "loss-cone" at the south pole in velocity space: stars inside this cone at pericenter are destroyed within one orbital period.

Far from the disruption loss-cone, those stars with $J_{max} \geq J \gg J_{min}$ are barely affected by the cone and distribute themselves nearly isotropically on the velocity sphere. However, near and inside the loss-cone, the stellar distribution is depleted. This depletion in velocity (or J) space drives a net flux of stars per unit energy, F_E, into the loss-cone from the ambient quasi-isotropic region. It is this J-space depletion and corresponding differential loss-cone flux that have been ignored in the naive 1-dimensional analysis described above.

Now consider how the stars move on the velocity sphere. In each period, stars experience a small rms change in angular momentum, j_2, due to gravitational encounters with their neighbors. This change causes them to move slightly on the velocity sphere, much like bees buzzing around a hive. What happens to those stars near the loss-cone depends critically on the ratio

$$q \equiv j_2^2/J_{min}^2(E) \tag{20}$$

which, in turn, depends on E. There are two extreme possibilities: (1) $q \ll 1$, in which case the change in J is sufficiently small that stars enter the loss-cone via two-dimensional diffusion. In this "empty loss-cone" case, the distribution function falls rapidly to zero at $J=J_{min}$ because any star found well inside the loss-cone would be destroyed in one period, long before it could be scattered out of the loss-cone; (2) $q \gg 1$, in which case the change in J is larger than the loss-cone opening so that most stars which reside inside the cone at apocenter manage to scatter out by the time they reach pericenter and are not disrupted. The distribution function remains nearly isotropic even inside the loss-cone in this "full loss-cone" case.

There exists a critical energy $E = E_{crit}$ defined by

$$q(E_{crit}) = 1 \tag{21}$$

Stars with energy E_{crit} typically reside at a radius

$$r_{crit} \sim GM/|E_{crit}| \tag{22}$$

from the black hole. This energy marks the transition between the "full" and "empty" loss-cone regimes.

Any attempt to analyze rigorously the two-dimensional character of the stellar distribution function $f(E,J)$ around a massive black hole must deal carefully with the disruption loss-cone region in phase space. In particular, numerical routines constructed to determine $f(E,J)$ must be able to handle stars reliably in the two opposite extreme regimes, $q \ll 1$ and $q \gg 1$ as well as handle stars in the critical transition regime in between. This realization was one of the

key factors governing the design of the 2+1 Monte Carlo simulation code
described below.

d)   The 2+1 Fokker-Planck Equation

The 2+1 Fokker-Planck equation for $F(E,J)$ is given by (Lightman and
Shapiro 1977; hereafter LS)

$$P(E)\frac{\partial f}{\partial t} = -\frac{\partial}{\partial E}\left\lceil f\varepsilon_1 \right\rceil + \frac{1}{2}\frac{\partial^2}{\partial E^2}\left\lceil f(\varepsilon_1^2 + \varepsilon_2^2) \right\rceil - \frac{1}{J}\frac{\partial}{\partial J}\left\lceil fJj_1 \right\rceil$$

$$+ \frac{1}{2J}\frac{\partial^2}{\partial J^2}\left\lceil fJ(j_1^2 + j_2^2) \right\rceil + \frac{1}{J}\frac{\partial^2}{\partial E\partial J}\left\lceil fJ(\varepsilon_1 j_1 + \zeta^2) \right\rceil ,$$

(23)

which must be solved in steady-state for the idealized problem formu-
lated in Section IV. In eqn. (23), ε_1 and j_1 are the mean changes in
energy and angular momentum per orbital period P, ε_2 and j_2 are the
dispersions about these means, and ζ^2 is the correlation between ε_2 and
j_2 for a star with fixed energy and angular momentum. These orbital
perturbations are obtained directly from the locally defined velocity
diffusion coefficients by integrating over orbits as shown in LS and in
Shapiro and Marchant (1978).
     Equation (23) is a 2+1 dimensional, integro-partial differential
equation. Its nonlinear character is "hidden" by the fact that the
orbital perturbations appearing in the equation are themselves
integrals over f.
     Consistent with the assumptions listed in Section IV, eqn. (23)
must be integrated subject to the following boundary conditions:
     i)   The distribution of unbound stars is isotropic and isothermal:
i.e. f satisfies

$$f = (2\pi v_0^2)^{-3/2} n_0 \exp(-E/v_0^2) \quad , \quad E > 0 \tag{24}$$

where v_0 is the constant line-of-sight velocity dispersion in the iso-
thermal core and n_0 is the core density.
     ii) The distribution function vanishes for $J > J_{max}$, i.e. $f = 0$
for $J > J_{max}$.
     iii) Stars are consumed by the black hole if and only if they lie
within the loss cone $\lceil J \leq J_{min}(E) \rceil$ when they are at <u>pericenter</u>; that
is, stars are destroyed when they are physically within the disruption
radius, $f = 0$, $r < r_D$.
     Note that (iii) is the precise statement of the loss-cone boundary
condition. It is not appropriate to replace (iii) by "simplifications"
such as $f = 0$ for $J < J_{min}$, which is not true in general (see Section
V.c).

In addition, eqn. (23) is subject to the initial (steady-state) condition

$$\frac{\partial f}{\partial t} = 0 \qquad\qquad (25)$$

e) Approximate Solution of Equation (23) and Scaling

Before discussing detailed Monte Carlo simulations of eqn. (23) for $f(E,J)$ it is useful to summarize the results of a crude analytic analysis of the two-dimensional problem by LS [see also Frank and Rees 1976]. Indeed, the availability of the analytic analysis and the scaling behavior which it predicted proved crucial to the construction of a reliable simulation code to solve the problem more accurately.

(1) <u>Bound Star Distribution (E < 0)</u>. LS found that the distribution could be written approximately in the power-law form of eqns. (4), (6) and (7), with

$$p \approx 1/4 + \text{logarithmic correction terms} \quad .$$

The correction terms are small except near r_D. Hence the solution of BW remained valid in the outer (observable) regions of the cusp.

(2) <u>Critical Radius</u>. The critical radius defined by eqn. (22) was found to satisfy

$$r_{crit}/r_a \approx 0.1 \; n_*^{-4/9} \; v_*^{32/9} \; M_3^{-20/27} \qquad (26)$$

where

$$n_* \equiv n_o/(5 \times 10^4 \; pc^{-3}) \quad \text{and} \quad v_* \equiv v_o/(10 \; km \; s^{-1}) \qquad (27)$$

and where $m = M_\odot$ and $r = R_\odot$. Thus one obtains the important result that r_{crit} resides <u>inside</u> the cusp for typical globular clusters with massive black holes (i.e. $r_{crit}/r_a < 1$) but <u>outside</u> the cusp for typical dense galactic nuclei (i.e. $r_{crit}/r_a > 1$ assuming $n_o \sim 10^7$ pc^{-3}, $v_o \sim 500$ km/s, $M \gtrsim 10^6 \; M_\odot$).

(3) <u>Loss-Cone Disruption Rate: Bound Stars (E < 0)</u>. The maximum possible star flux that a relaxed system can accommodate is, on dimensional grounds,

$$F_{max}(r) \sim \frac{n(r) \; r^3}{t_r(r)} \qquad\qquad (28)$$

where t_r is the local relaxation timescale. LS found that the differ-
ential loss-cone disruption rate F_E (stars/time/specific energy)
peaked sharply at E_{crit} and that the total disruption rate satisfied

$$F \equiv \int_{-M/r_D}^{0} F_E\ dE \sim F_{max}(r_{crit})/\ln\ (r_{crit}/r_D) \tag{29}$$

$$\sim 10^{-7}\ n_*^{14/9}\ v_*^{-49/9}\ M_3^{61/27}\ yr^{-1}\ , \tag{30}$$

where we have neglected logarithmic variations in eqn. (29). The cor-
responding core heating rate due to disruption was found to be

$$E \equiv \int_{-M/r_D}^{0} F_E\ |E|\ dE \sim F \left(\frac{GM}{r_{crit}}\right) \ln\ (r_{crit}/r_D) \tag{31}$$

(4) Loss-Cone Disruption Rate: Unbound Stars (E>0). Unbound stars
can also enter the loss-cone at pericenter and be disrupted. Their
rate of disruption was found to be

$$F^u \approx F\ (r_{crit}/r_a)^{5/4}\ . \tag{32}$$

Accordingly, the bound star disruption rate dominates the unbound rate
for typical globular clusters but the reverse is true for dense
galactic nuclei. A similar result applies to the relative heating
rates, although for unbound stars, is negative and corresponds to
core "cooling":

$$E^u \approx v_o^2\ F^u\ . \tag{33}$$

f) Time-Dependent, Homological Core Evolution.

Suppose we remove the assumption of steady-state. How will a relaxed
cluster core respond with time to the presence of a central black hole?
This question motivated Shapiro (1977) to construct a simple homologi-
cal model for the evolution of a globular cluster core with a central
hole. The equations were those employed by Ambartsumian (1938) and
Spitzer (1940) in their simple "evaporation model" for core collapse,
modified by terms accounting for the effects of a central hole. The
key effects considered were the tidal disruption of bound stars by the
hole (eqn. 28) and the associated heating of the core which accompanies
this process (eqn. 31).

The resulting evolution of the cluster core radius with time is shown in Fig. 3 for various initial black hole masses. In all cases, the hole eventually manages to halt and reverse core collapse. At late times the core expands asymptotically to infinity according to

$$R_c \propto t^{2/3} \quad , \quad t \to \infty \quad . \tag{34}$$
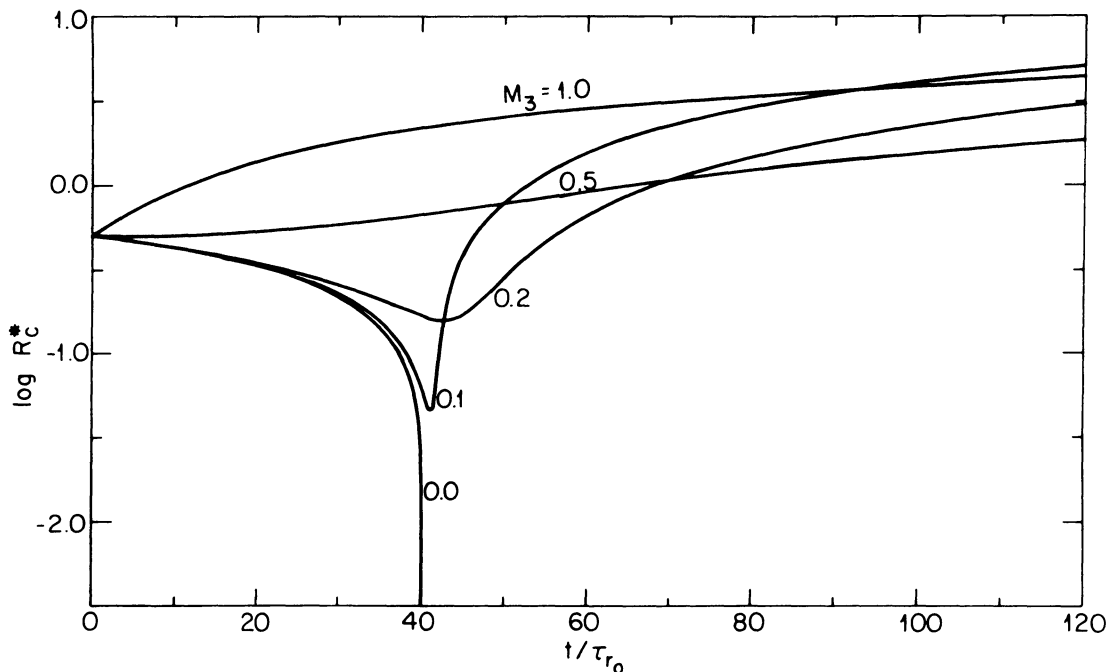
Figure 3: The core radius R_c^* as a function of time t (in units of the initial relaxation time $\tau_{r_0} = 6.2 \times 10^6$ yr) for a cluster with an initial core density $n_{c_0}^* = 0.2$, radius $R_c^* = 0.5$, and black hole mass M_3 between 0 and 1. Core parameters are expressed in the following non-dimensional units: $n_c^* = n_c/(5 \times 10^4 \text{ pc}^{-3})$, $R_c^* = R_c/(1 \text{ pc})$, $M_3 = M/(10^3 M_\odot)$. Massive central black holes invariably halt and reverse core collapse. From Shapiro (1977).

This behavior is thus quite analogous to that found by Hénon (1961; 1975) for cluster cores heated by central binaries. In spite of the crudeness of the homological model, it does suggest that core re-expansion may be a generic feature of post-collapse evolution, whatever the central energy source. It also points to the dissolution of a globular cluster in the Galactic tidal field as a plausible final outcome (Wielen 1971; Shapiro 1977).

VI. THE MONTE CARLO APPROACH

a) Key Numerical Difficulty: The Problem of Multiple Lengthscales

Simulating the full 2D problem rigorously by means of a Monte Carlo
scheme immediately poses some "technical" difficulties. The key diffi-
culties are associated with the vast dynamical range spanned by the
parameters describing a relaxed cluster with a massive, central hole.
This large dynamical range is in turn due to the existence of multiple,
widely disparate length scales characterizing such a system. In this
respect, a star cluster containing a massive black hole is not unlike
many other multidimensional, nonlinear, many-body systems whose dynami-
cal behavior on large scales requires detailed knowledge of behavior on
small scales, and vice versa.

Specifically, consider the idealized problem posed in Section IV
and focus on the bound stars $(E < 0)$. They occupy the region $r_D \lesssim r \lesssim r_a$, which spans over six decades in radial coordinate space and a
corresponding six decades in $|E| \sim GM/r$ phase space. The associated
number density of stars in the cusp, $N(E) \propto |E|^{-9/4}$ thus decreases by
over 14 decades through the cusp! This fact poses the following
numerical challenge: how do we achieve statistical reliability at high
$|E|$ deep in the cusp with only a finite number of stars at low $|E|$ at
the outer edge of cusp?

Consider next the position of bound stars in J-space. They occupy
the region $J_{min}(E) \lesssim J \lesssim J_{max}(E)$, where the ratio J_{min}/J_{max} varies
between $(r_D/r_a)^{1/2} \sim 10^{-3} \lesssim J_{min}/J_{max} \lesssim 1$. The small value of this
parameter, which describes the "opening angle" of the disruption loss-
cone, throughout most of the cusp poses the problem: how do we achieve
accuracy near the relatively small loss-cone to enforce the all-
important tidal disruption boundary condition?

Now consider the time variable. We first note that in a relaxed
Fokker-Planck system, it is not so much dynamical or orbital time, t_d
which matters but "only" the ratio of t_d to the local relaxation time,
t_r. But even so, this ratio scales like $t_d/t_r \sim |E|^{-5/4}$ in the cusp
and thus varies between $10^{-11} \lesssim t_d/t_r \lesssim 10^{-4}$. This vast variation
poses the problem: how do we follow stars for many orbital periods -
some for many more than others, depending upon $|E|$ - before they relax?

Finally note that only the bound stars entered into the above
considerations. For general problems where the unbound star distribu-
tion is not fixed, a whole new set of lengthscales (e.g. core radius,
Galactic tidal radius, etc.) enter the discussion and increase the
dynamical range of the system even further!

b) Confronting the Difficulty

Below we summarize some of the tricks we have incorporated in our 2+1
Monte Carlo simulation scheme to handle the problem of multiple length-
scales. As these tricks, as well as the problems they are designed to
overcome, are quite general in character, it may prove useful to in-
corporate them in other simulation codes.

Before discussing them we first note that the highly nonlinear
character of the Fokker-Planck equation is treated by the familiar
pseudo-linearization device of following a 'test' star distribution
which relaxes by scattering not against itself directly, but against a
fixed 'field' star background distribution (cf. Chandrasekhar 1942;
Spitzer 1962). Of course, the 'field' star distribution and the
orbital perturbations it induces are recomputed at regular time inter-
vals to match the evolving 'test' star distribution, thereby achieving
self-consistency (see Box 2).

Box 2
MONTE-CARLO SIMULATIONS IN (E,J) SPACE
'FIELD' STARS vs 'TEST' STARS

```
                    ( start )
                        │
                    ( t = t₀ )
                        │
        ┌───────────────────────────────────┐
        │  choose initial 'field' star distribution │
        │            f = f (E, J, t₀)              │
        └───────────────────────────────────┘
                        │
        ┌───────────────────────────────────┐
        │ distribute initial 'test' stars in E-J bins: │
        │  N (E, J, t₀) = 8π² J P(E,J) f(E, J, t₀)    │
        └───────────────────────────────────┘
                        │
        ┌───────────────────────────────────┐
        │             isotropize f :             │
        └───────────────────────────────────┘
```

$$\bar{f}\,(E,t) = \tfrac{1}{2}\, J_{max}^{-2}\,(E) \int_0^{J_{max}} f(E,J,t)\, J dJ$$

```
        ┌───────────────────────────────────┐
        │ tabulate diffusion coefficients on E-J grid using f̄ │
        │        f̄ ⟹ ε₁, ε₂, j₁, j₂, ζ                │
        └───────────────────────────────────┘
                        │
        ┌───────────────────────────────────┐
        │          evolve 'test' particles:         │
        │  E → E + ΔE,  J → J + ΔJ,  t → t + Δt   │
        └───────────────────────────────────┘
                        │
        ┌───────────────────────────────────┐
        │ bin 'test' particles and get new 'field' │
        │          particle  distribution :         │
        │  f(E,J,t) = [8π²J P(E,J)]⁻¹ N(E,J,t)    │
        └───────────────────────────────────┘
                        │
                ( t ≥ t_final ? )
              no │         │ yes
                 │       [ stop ]
```

We employ one approximation in our application of the method: the
orbital perturbation coefficients, which control the motions of 'test'
stars in phase space, are computed from the J-averaged (isotropized)
field-star distribution. This approximation is reasonable whenever the
field-star distribution does not vary greatly from isotropy, as is the
case in the black hole problem.

Box 3

PARTICLE 'CREATION - ANNIHILATION' SCHEME :

"DYNAMICAL RENORMALIZATION"

'Test - star' Energy - level diagram:

'creation - annihilation' boundary

'parent' (weight : 1)

create
N 'clones' (weight : $1/N$)

$\log |E|$

annihilate all but $1/N$

(to BH)

⟨dashed circle⟩ particles at t

⟨hatched circle⟩ particles at $t + \Delta t$

"Put particles where you need them"

---
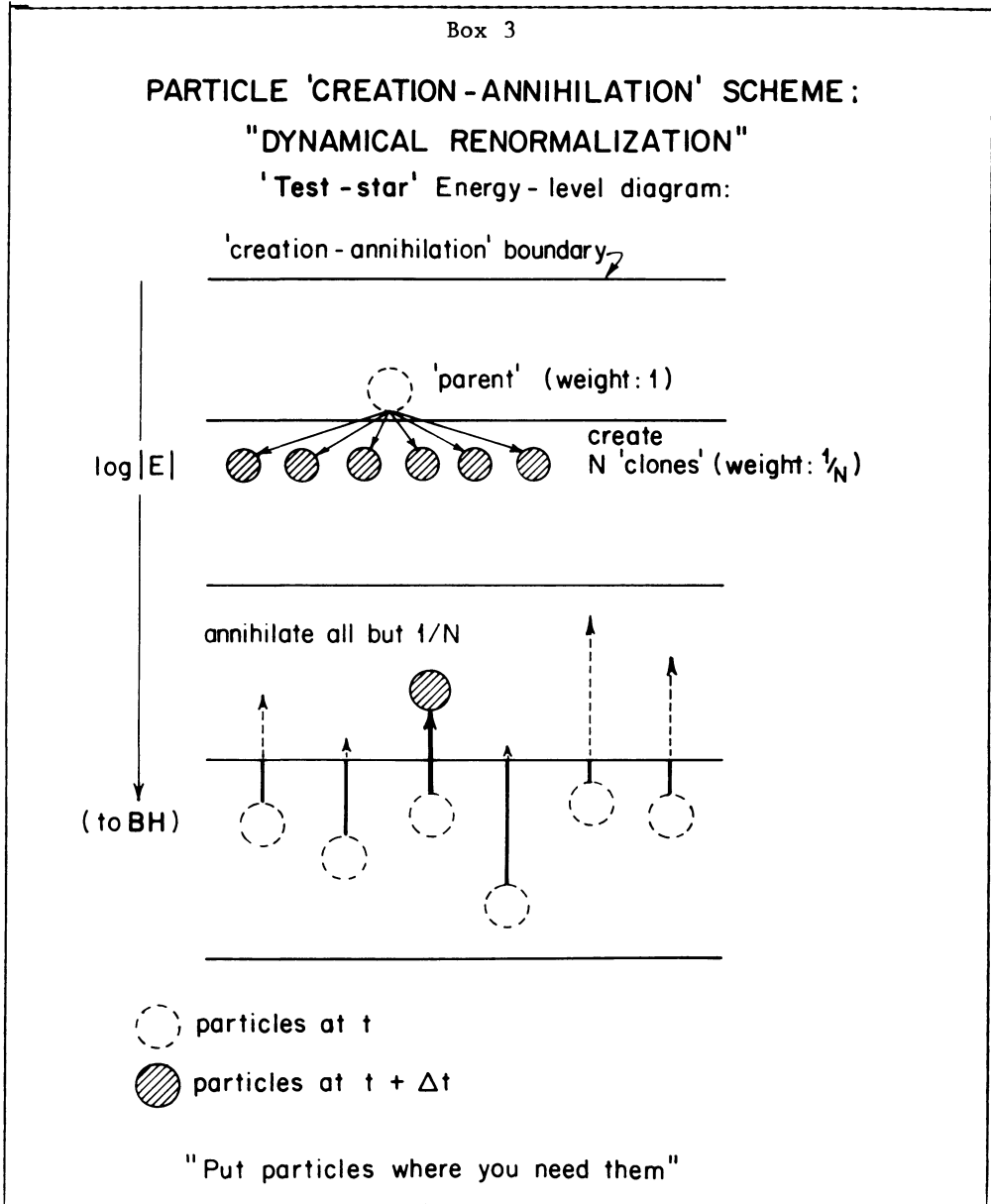
1) <u>Particle 'Creation-Annihilation' Scheme</u>. To provide sufficient
numbers of test stars and thereby guarantee statistical reliability in
low populated regions of phase space (e.g. high $|E|$ regions in the
cusp) we construct a particle 'creation-annihilation' scheme, illus-
trated schematically in Box 3. Specifically, at predetermined
boundaries in E-space, stars diffusing toward higher $|E|$ generate
"clones" which may, themselves, subsequently diffuse toward the black
hole independently of their "parent". To prevent artificial numerical
contamination, these clones are prevented from crossing back across the
energy boundary below which they formed, and, instead, are removed from
the system if they attempt to do so. Since all test stars are dynami-
cally coupled and interact only with field stars, there is no nonlinear
feedback associated with this procedure.

     Our method for accurately surveying many decades in phase space by
particle 'cloning' has much in common with the Renormalization Group
applied elsewhere in many-body physics. Accordingly, we sometimes
refer to our procedure as 'Dynamical Renormalization'.

2) <u>'Time-step Adjustment' Scheme</u>. To reconcile the very short
dynamical timescales t_d associated with loss-cone consumption, with the
rather long timescales associated with 2-body relaxation, $t_r \gg t_d$, we
employ a 'time-step adjustment' algorithm (Box 4). That is, the size
of an individual test particle time-step is determined by the parti-
cles' value of E and J. For <u>typical</u> stars, it is chosen to be some
fraction of the local relaxation timescale and consists of many orbital
periods (the number increasing as $|E|^{5/4}$ in the cusp). However, for
stars on <u>critical</u> trajectories (e.g. near the disruption loss-cone),
the step size is chosen to be an orbital period so that the stars'
position can be examined each time they reach pericenter. The ability
to chose whether or not to follow a star on an orbital timescale gives
maximum flexibility and efficiency to any Fokker-Planck simulation
scheme.

VII. MONTE CARLO SIMULATIONS OF BLACK HOLES IN GLOBULAR STAR CLUSTERS

(a) Simulations of the Idealized Problem

Figure 4 shows the nondimensional, isotropized distribution function
and differential tidal disruption rate for bound stars obtained by
Shapiro and Marchant (1978) using the E-J Monte Carlo simulation
scheme. The isotropized profile is quite comparable to the 1D BW
profile except that deep in cusp near the disruption region
$(x_D \equiv M/(2r_D v_o^2)) = 10^4$ in the case illustrated) considerable depletion
is evident. A nearly identical isotropized profile to the Monte Carlo
one shown here was obtained by Cohn and Kulsrud (1978), who integrated
the 2D Fokker-Planck equation by finite-difference techniques.

Box 4

'TIME STEP ADJUSTMENT' ALGORITHM

$n = n(E, J) = $ number of orbital periods per Monte-Carlo time-step; guarantees $\Delta E / E$ and $\Delta J / J$ are $\ll 1$.

a. "Typical" bound stars : $J \lesssim J_{max}$ (E)
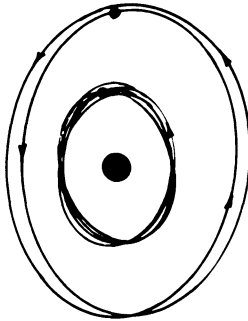
$$n \propto \frac{t_r}{t_d} \propto |E|^{5/4} \propto r^{-5/4}$$

● tidal disruption sphere

b. Stars near 'loss-cone': $J \ll J_{max}$ (E)
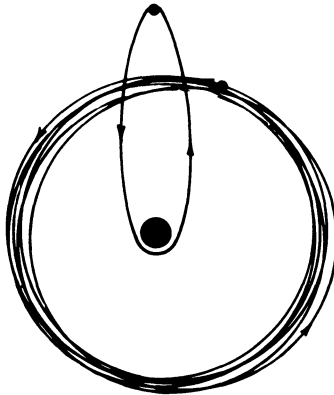
$$n \propto \left(\frac{J}{J_{max}}\right)^2$$

∴ For <u>typical</u> stars each step constitues many periods

BUT

stars on <u>critical</u> trajectories (i.e. "loss-cone" orbits) can be followed carefully on orbital timescales.

The region of maximum tidal disruption, as measured by $|E|F_E$, is
strongly peaked near E_{crit}, as predicted by LS (see Section V.e). In-
deed, most qualitative aspects of the solution discussed by LS, includ-
ing the scaling, are verified by the numerical simulation.
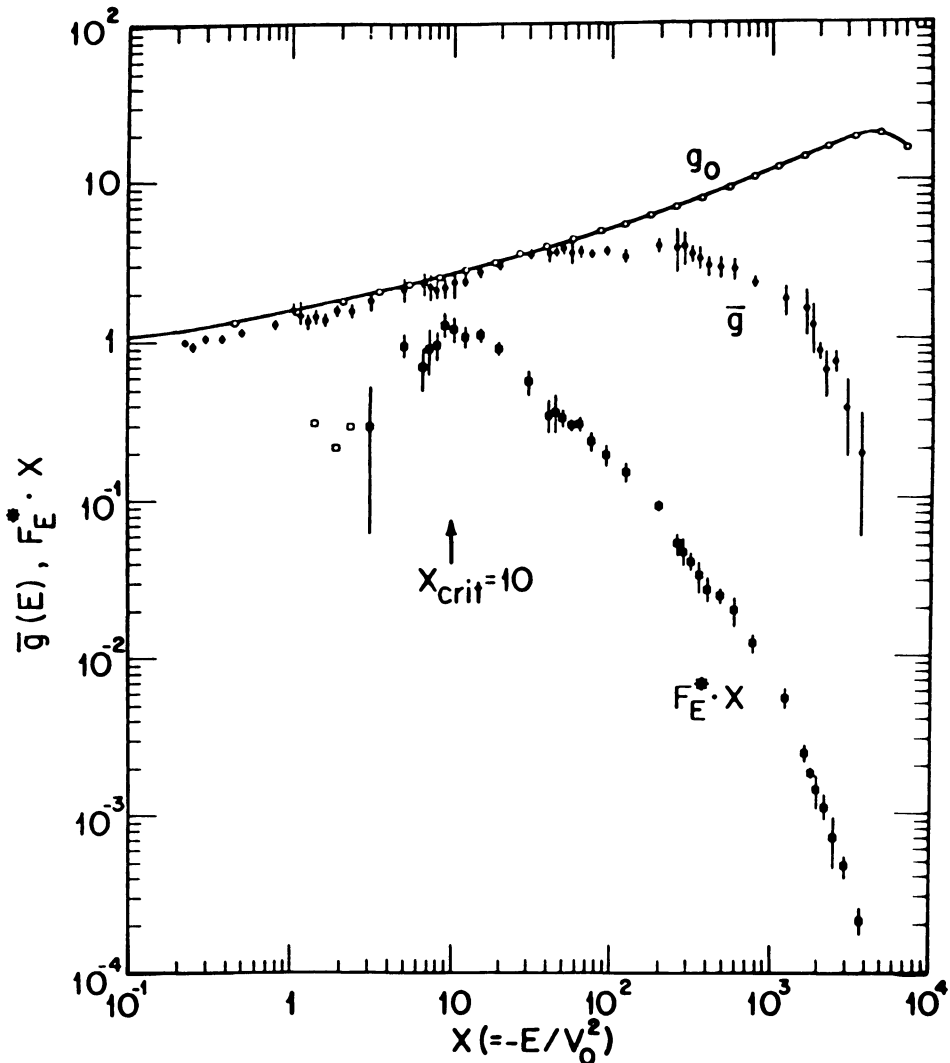
Figure 4: The isotropized distribution function, $\overline{g}$, for the case
x_{crit} = 10 and x_D = 10^4, is plotted as a function of dimensionless
energy $x \equiv -E/v_o^2$ (filled circles). The function $\overline{g}$ is normalized to
unity at x = 0. The differential consumption rate, $F_E^* x$, is also
plotted (filled squares); and those data points which had rather large
error bars are distinguished (open squares). The function $F_E^* x$ peaks
sharply near x_{crit}, indicating that the black hole principally consumes
stars of energy ~ E_{crit}. The distribution g_o is the (one-dimensional)
BW solution (solid line). From Shapiro and Marchant (1978).

(b)   Simulations of Black Holes in Realistic Clusters

The Monte Carlo scheme was used by Marchant and Shapiro (1979) to
determine the steady-state distribution and tidal disruption rate of
stars around a massive black hole at the center of a <u>realistic</u> King-
model stellar cluster. Here, the <u>self-gravity</u> of the stars is taken
into account. The density and surface density profiles calculated for
different assumed black hole masses are plotted in Figs. 5 and 6,
respectively. For these computations the total cluster mass is
$M_{cluster} = 3.6 \times 10^5\ M_\odot$ and the core mass is $M_{core} = 2 \times 10^4\ M_\odot$. It is
clear from the figures that self-gravity becomes important whenever the
black hole mass is sufficiently large: $M/M_{core} \gtrsim 0.1$. In this limit
the cusp does not display any distinctive structure near r_a. Thus if
such high-mass black holes reside in globular clusters, their main
observable signature might be the lack of a resolvable cluster core.
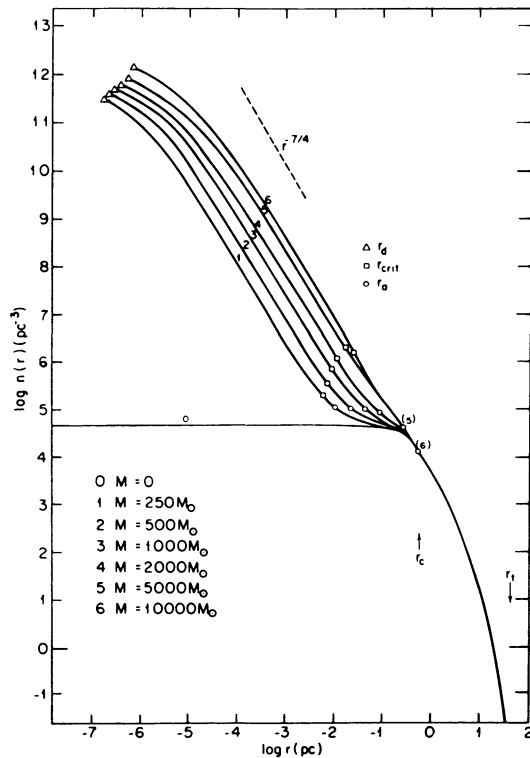
Figure 5:   Density of stars n is plotted as a function of cluster
radius r for clusters with black holes with different assumed masses M.
The ambient King-model cluster parameters are $N = 3.6 \times 10^5$ stars, $v_0 =$
10 km s^{-1}, and $\phi_s(0) = -8v_0^2$. The cluster tidal radius r_t, the core
radius r_{crit}, and the tidal disruption radius r_d, are shown for all
cases. All the black-hole cases show cusp profiles similar to the
$r^{-7/4}$ power law. The effects of self-gravity near r_a are evident for
the very massive black-hole cases. From Marchant and Shapiro (1979).
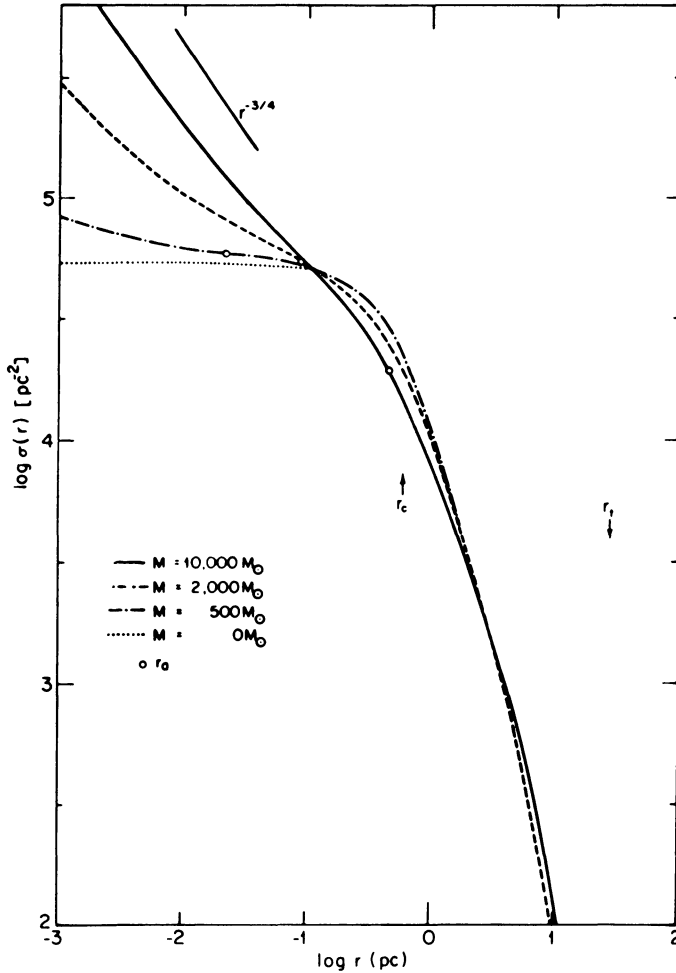
Figure 6: Surface density of stars σ as a function of the projected cluster radius r for some of the clusters shown in Figure 5. Note that the case M = 10^4 $M_\odot$ shows no shoulder in its surface-density profile. In all cases, the distinctive $r^{-3/4}$ dependence of σ is evident, but only well inside the accretion radius. From Marchant and Shapiro (1979).

c) 2+1 Cluster Evolution Simulations

By far the most significant application of the 2+1 Monte Carlo scheme is determining the detailed, time-dependent, dynamical evolution of a realistic star cluster containing a massive, central black hole. Such calculations were performed by Marchant and Shapiro (1980) and Duncan and Shapiro (1982).

To check how well the simulation scheme could track Fokker-Planck evolution, the dynamical evolution of a cluster without a central hole was considered first. Initial data for this case consisted of a Plummer model (n = 5 polytrope) allowing for a finite Galactic tidal cut-off radius r_t. In general, the familiar features of the 'gravo-thermal catastrophe' were revealed by our integrations. Specifically, the simulations of the early and intermediate phases of core collapse, $0 \leq t/t_{rh} \leq 13.4$, agreed well with earlier 2+1 Fokker-Planck simulations of Spitzer and his colleagues [see paper by Spitzer in these Proceedings for a review and references]. Here t_{rh} is the initial half-mass relaxation time defined by Spitzer. Our simulations of the late phases, $13.4 \leq t/t_{rh} \leq 14.7$, agreed well with the Fokker-Planck integrations of Cohn (1979, 1980). In particular, the homologous nature of advanced core collapse as predicted by Lynden-Bell and Eggleton (1980) was verified. Not surprisingly, it was found to be relatively independent of r_t.
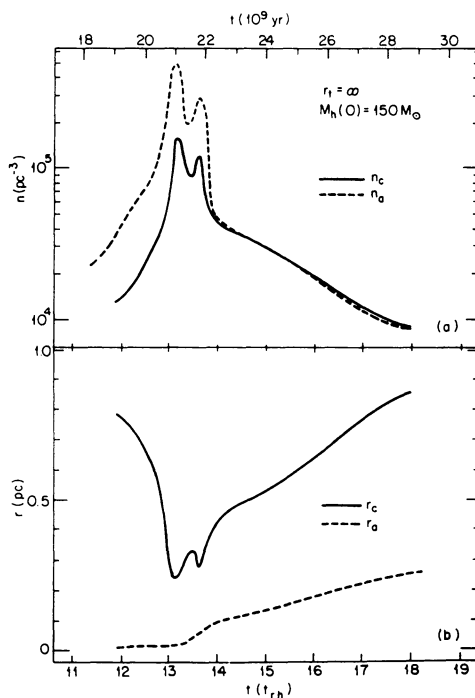
Figure 7: (a) The density at r_a, $n_a \equiv n(r_a)$ (dashed line), and the core density n_c as functions of time. (b) The core radius R_c (solid curve) and the accretion radius r_a as functions of time. From Duncan and Shapiro (1982).

Confident that our scheme could handle evolution accurately, we next considered the effect of a central black hole. The initial data again consisted of a Plummer model with a finite tidal radius, but now

we inserted a black hole, with initial mass in the range
$0 \leq M_i/M_\odot \leq 2000$ at the cluster center at an arbitrary time t_i (which
we varied) during the cluster's evolution. We found that in all cases
core collapse is eventually reversed by the heat flux from stellar dis-
ruption by the hole. The system attains a quasi-stationary, expanding
state, by which time the hole (if assumed to swallow most of the dis-
rupted stellar debris) has grown to several thousand solar masses.
This expanding state appears to be roughly independent of (i) the
initial hole mass, (ii) the time during core evolution at which the
hole is introduced and, (iii) the value of r_t.

  Figure 7 illustrates the variation with time of characteristic
central densities and radii during the evolution. Core collapse,
followed by re-expansion, are clearly evident. The corresponding
growth of the black hole is shown in Fig. 8. Typically, core bounce
occurs when the hole grows to $M \approx 0.1\, M_{core}$.
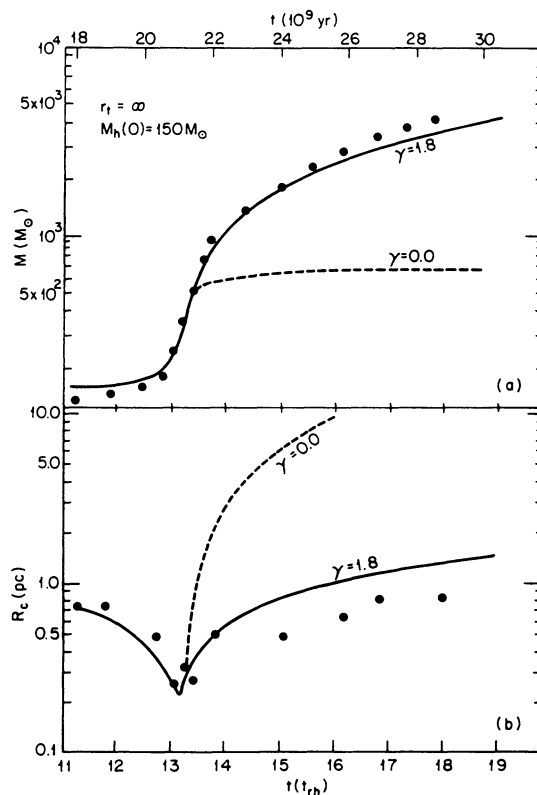
Figure 8:   (a) The growth of the black hole mass M_h with time for the
case shown in Fig. 7. The filled circles are "data" from a Monte Carlo
simulation, while the smooth curves represent homological solutions
characterized by one free parameter (γ). (b) The time evolution of the
core radius. From Duncan and Shapiro (1982).

VIII. MONTE CARLO SIMULATIONS OF BLACK HOLES IN DENSE GALACTIC NUCLEI

Dense galactic nuclei may provide more hospitable environments than globular clusters for forming massive black holes. Indeed, many models of AGN's and quasars now favor the presence of a supermassive black hole ($M \gtrsim 10^6$–$10^9 \, M_\odot$) to power these energetic sources (see Table 2). It was therefore natural for Duncan and Shapiro (1983) to extend their 2+1 Monte Carlo simulation scheme to study the dynamical evolution of a dense galactic nucleus with a massive, central hole.

As initial data they considered King model clusters of solar-type stars. The core parameter for these models were in the range expected for AGN's and quasars,

$$2 \times 10^7 \leq M_{core}/M_\odot < 3 \times 10^8$$

$$300 \leq v_o \ (km/s) < 10^3 \tag{35}$$

$$10^6 \leq n_o \ (stars \ pc^{-3}) < 10^7 \ ,$$

while the initial central black hole mass was varied between

$$2 \times 10^6 < M/M_\odot < 5 \times 10^4 \quad . \tag{36}$$

In addition to tidal disruption by the black hole, stars in dense galactic nuclei can be destroyed by star-star collisions. These collisions were incorporated in the Monte Carlo simulations, where it was assumed that the stars disrupted immediately upon impact and that all the gaseous debris liberated during collisions and tidal disruptions is consumed by the central hole. Accordingly, the hole grows at a rate given by

$$\dot{M} = m \, (F_{coll} + F_{tide}) \quad . \tag{37}$$

This accretion by the hole results in a radiation luminosity given by

$$L = 7 \times 10^{45} \left(\frac{\varepsilon}{0.1} \right) \left(\frac{\dot{M}}{M_\odot \ yr^{-1}} \right) \ erg \ s^{-1} \tag{38}$$

where ε is the assumed conversion efficiency of rest mass into radiation.

The key results of this study were the following:

1. Star destructions result predominantly from <u>collisions</u> when the rms velocity v_0 exceeds the escape velocity $v_{esc} \approx \overline{620 \text{ km}}/\text{s}$ from a star. Destructions result predominantly from <u>tidal disruptions</u> when the reverse is true.

2. The <u>maximum</u> stellar destruction rate achieved in these systems is found to be

$$m \; F_{tide}(\text{max}) \; \sim \; \frac{M_{core}}{t_r} \; \lesssim \; 10^{-2} \; M_{\odot} \; \text{yr}^{-1} \tag{39}$$

for tidal disruption and

$$m \; F_{coll}(\text{max}) \; \sim \; \frac{M_{core}}{t_{coll}} \; \sim \; M_{\odot} \; \text{yr}^{-1} \tag{40}$$

for star collisions. Here t_r and t_{coll} are the core relaxation and collision timescales, respectively, and the numerical values were those found for the Monte Carlo simulations (they are largely determined by the assumed initial conditions).

Equations (37)–(40) thus suggest that quasars (L ~ 10^{45}–10^{48} erg s^{-1}) may be dense galactic nuclei in which physical collisions are occurring, while AGN's (L ~ 10^{42}–10^{45} erg s^{-1}) may be nuclei where collisions are unimportant and tidal disruptions dominate. Similar conclusions have been reached by other investigations (see references in Box 1).

3. For late times, $\dot{M}$, hence L, decays like

$$L \; \sim \; \dot{M} \; \sim \; t^{-\alpha} \tag{41}$$

where α depends on the power-law stellar profile outside the core and is, typically, in the range $\alpha \sim 0.8 - 1$.

Simulation results for a candidate "quasar" model are shown in Figs. 9 and 10. In Fig. 9 the evolution of the density profile is shown. For this case the initial core relaxation time is $t_{r,i} = 4.5 \times 10^9$ yr while the collision time is $t_{coll,i} = 2 \times 10^8$ yr; evidently $t_{coll,i} \ll t_{r,i}$ so collisions dominate. In this case the bound stars in the cusp are quickly destroyed by collisions, leaving only the unbound stars with a characteristic $n(r) \propto r^{-1/2}$ profile. In Fig. 10 the black hole consumption rate is plotted vs time. This rate remains constant for $t \lesssim t_{coll,i}$ while the core is being consumed, after which it decays
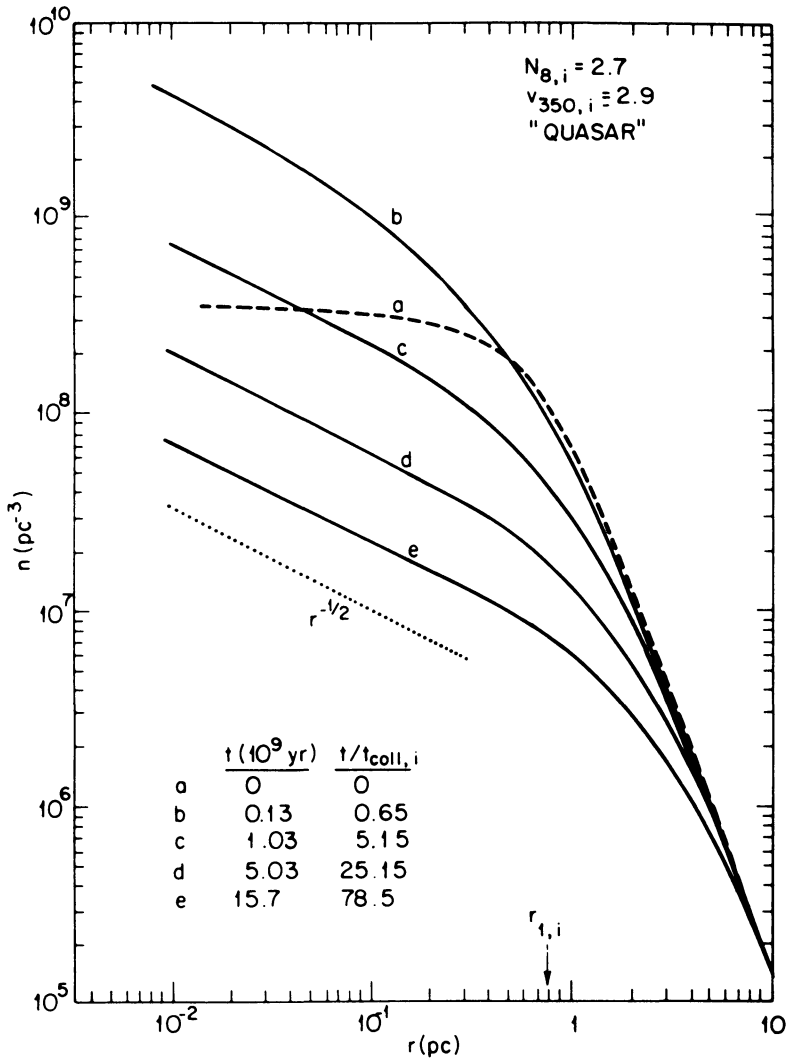
Figure 9: The stellar density profile at five successive times for the "quasar" model simulation. The dashed curve shows the initial profile, while the lowest solid curve is the profile at the end of the simulation. The initial cluster has a core radius $r_{1,i}$, star number $N_{8,i}$ and line-of-sight velocity dispersion $v_{350,i}$. From Duncan and Shapiro (1983).

like t^{-1} as the hole eats its way out into the halo. From an initial mass of 2×10^6 $M_\odot$, the black hole grows to 3×10^9 $M_\odot$ by the end of the simulation. The maximum luminosity achieved during the cluster's evolution is about $L \sim 10^{46}$ erg s^{-1} (for $\varepsilon = 0.1$), which is quite re-spectable for a typical quasar.
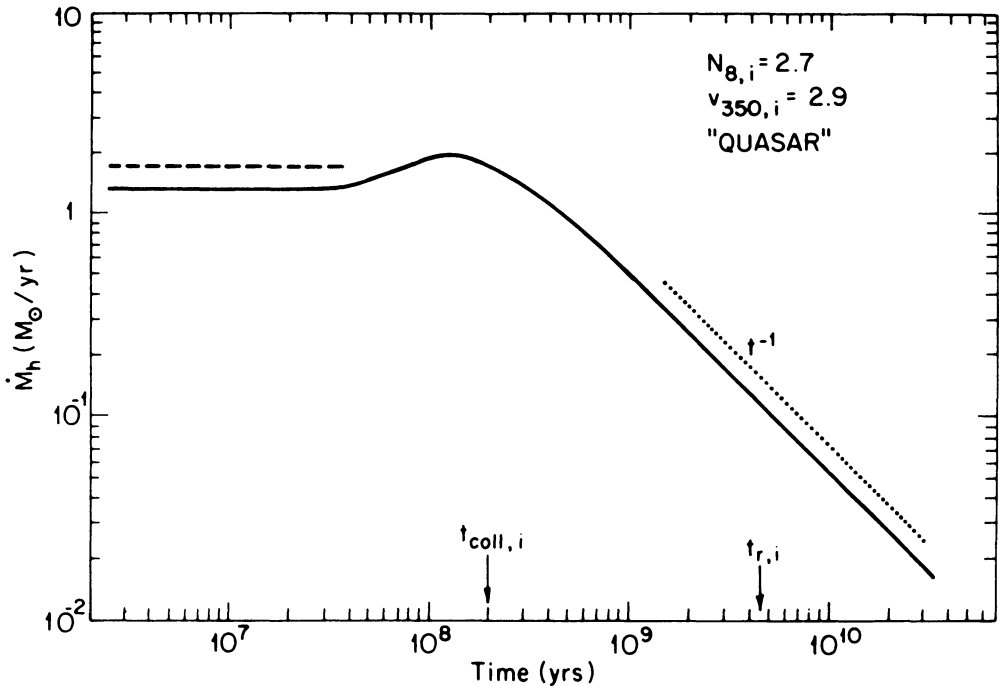
Figure 10:   The black hole growth rate $\dot{M}_h$ ($\propto$ L) as a function of time for the case shown in Fig. 9.   The <u>dashed</u> curve is the rate predicted by simple analytic arguments.   From Duncan and Shapiro (1983).

IX.   THE BIRTH OF SUPERMASSIVE BLACK HOLES VIA THE COLLAPSE OF DENSE STELLAR SYSTEMS

An analysis of massive black holes in star clusters would not be complete without some discussion of their origin. A possible scenario for the formation of massive holes in globular clusters via star colli- sions and coalescence has been proposed by Spitzer (1975) and sketched by Lightman and Shapiro (1978) (see Section II.a).   Such a mechanism cannot produce black holes much more massive than ~ 100 $M_\odot$, but we have seen that black holes in clusters can grow considerably by the consump- tion of tidally disrupted stars (Section VII.c).   This scenario has to be investigated in much greater detail before its likelihood can be properly assessed.

Several mechanisms have been suggested for the formation of supermassive black holes in dense galactic nuclei (see Box 1).   One of the most appealing is the scenario first put forward by Zel'dovich and

Podurets (1965). They argued that the combined effects of secular core collapse (i.e. the 'gravothermal catastrophe', which they referred to as 'stellar evaporation') and star-star collisions would drive a cluster to states of ever higher central velocity and redshift. At sufficiently high redshift, the cluster would become relativistically unstable, at which point it would undergo catastrophic collapse on a dynamical timescale to a supermassive black hole. They had in mind initial Newtonian star clusters composed of stellar mass black holes which would thus ultimately collapse to form a single, supermassive black hole.

Some recent theoretical developments suggest that this proposal by Zel'dovich and Podurets (1965) ought to be regarded quite seriously. For the first time, it has been possible to integrate numerically the full Einstein field equations for an arbitrary spherical, collisionless gas in General Relativity (Shapiro and Teukolsky 1985 a,b). These integrations enable one to follow on the computer the evolution on dynamical timescales of relativistic star clusters, even during epochs characterized by total gravitational collapse and the formation of supermassive black holes. The formation and growth of the black hole can be followed accurately without the appearance of numerical or physical singularities.

The original speculation of Zel'dovich and Podurets (1965) that star clusters become relativistically unstable at sufficiently high central redshift ($z_c \gtrsim 0.5$) has been demonstrated rigorously in perturbation theory (see, e.g., Ipser 1969, 1980; Fackerell, Ipser and Thorne 1969 and references therein). The recent numerical integrations described above provide further verification of this relativistic instability and, more significantly, follow its nonlinear growth and the ultimate fate of unstable clusters. In particular, the integrations show quite generally that clusters of sufficiently high central redshift do undergo catastrophic collapse to a black hole on a dynamical timescale. Moreover, they reveal that, while the core may encompass only a small fraction of the cluster mass at the center initially, the hole ultimately grows to entrap virtually the entire cluster in a few mean orbital periods.

The fully relativistic, Vlasov simulations of spherical star clusters described above provide fresh support for the Zel'dovich and Podurets supermassive black hole scenario. They have motivated Shapiro and Teukolsky (1985c) to reconsider this suggestion in greater detail, in light of our current knowledge of dense galactic nuclei, the gravothermal catastrophe, etc. The result is summarized in Fig. 11. Illustrated are the evolutionary tracks of initially Newtonian, isothermal cores of dense stellar systems composed of neutron stars ($m = 1.4 \, M_\odot$). At any instant, the cores are defined by two parameters: N_c, the total number of core stars and z_c, the central redshift in the core ($z_c \propto \Phi_c \propto v_c^2$, where Φ_c is the central potential and v_c is the core velocity dispersion, also shown). Each track is composed of two distinct segments, corresponding to two different epochs: an early, low-redshift ($z < z_{coll}$) "point-mass" epoch during which the core undergoes secular collapse via the 'gravothermal catastrophe' and a later,
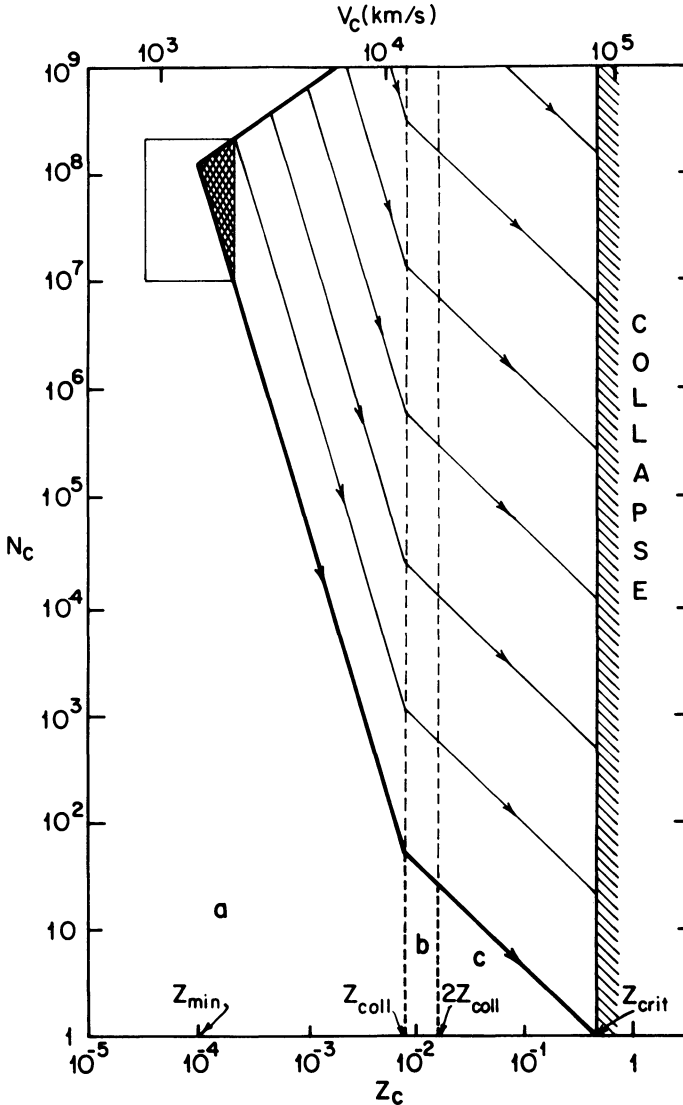
Figure 11:   Dynamical evolution tracks in the N_c - z_c plane of dense cluster cores consisting of 1.4 $M_\odot$ neutron stars. During phase (a), the "gravothermal catastrophe", the core evolves by two-body scattering to central redshift z_{coll} ~ 8 × 10^{-3}. During phase (b) the neutron stars collide, coalesce and collapse to form ~ 2.8 $M_\odot$ black holes. During phase (c) the remnant black holes collide and coalesce, driving the core to central redshift z_{crit} ~ 0.5. At this point the entire cluster becomes relativistically unstable and undergoes catastrophic collapse to a supermassive black hole in a few mean orbital periods. The range of plausible core parameters for dense galactic nuclei lie in the box shown in the upper left of the figure. The hatched region shows the fraction of these capable of evolving to a supermassive black hole in a Hubble time. From Shapiro and Teukolsky (1985c).

high-redshift ($z > z_{coll}$) "finite-radius" epoch during which star-star collisions and coalescences dominate the evolution. During both epochs, the number of core stars decrease while the central redshift increases. Ultimately, the core achieves relativistic central velocities and redshift ($z = z_{crit} \sim 0.5$) at which point it undergoes total gravitational collapse to a black hole. The hole quickly grows outward and eventually swallows up most of the ambient cluster in a few mean dynamical timescales.

Only those clusters which can evolve to a relativistic state in a Hubble time are relevant for our investigation. Also, only those clusters which have more than one star remaining in their core by $z = z_{crit}$ can actually reach this state. These two constraints confine the tracks to be within the heavy lines in the figure. A similar figure can be drawn for clusters consisting initially of white dwarfs or stellar-mass black holes.

Consider the consequences of this scenario. First, there is minimum central redshift ($z = z_{min} \sim 10^{-4}$) or a minimum central velocity dispersion ($v_c \sim 10^3$ km s^{-1}) below which a cluster of neutron stars cannot evolve to a relativistic state in a Hubble time. Although this minimum core velocity is large, it is not unreasonably large for conditions expected in dense galactic nuclei. Indeed, consider the range of plausible parameters calculated for dense galactic nuclei following the collision-coalescence epoch which the normal stars in the nucleus are expected to undergo (Colgate 1967; Sanders 1970). Very likely, this initial collision-coalescence epoch will convert the dense, but otherwise normal galactic nucleus into a cluster of stellar-mass compact stars - black holes or neutron stars (Begelman and Rees 1978). The parameter range calculated by Colgate (1967) and Sanders (1970) for such systems is indicated by the box in the upper left-hand corner of Figure 11. What is interesting is that (1) this box intersects a small, but finite domain occupied by those dense cores capable of evolving to supermassive black holes in a Hubble time and (2) the domain of intersection occurs in the range $10^7 \lesssim N_c \lesssim 10^8$, indicating that, following total gravitational collapse, the clusters will yield supermassive black holes with masses in the range $10^7 \lesssim M/M_\odot \lesssim 10^8$. This is roughly the mass range of black holes which can generate AGN and quasar luminosities via gas accretion near the Eddington limit! It is thus within the mass range frequently cited in black hole models of such systems (cf. Section VIII).

The supermassive black hole generation mechanism in dense clusters discussed here is attractive and uncomplicated. It leads to black holes of the "right size" to explain quasars and AGNs. Whether or not the picture is also correct will depend on the results of more detailed, future studies, both theoretical and observational.

REFERENCES

Ambartsumian, V.A. 1938, Ann. Lenningrad State Univ. No. 22, (Astr. Series, Issue 4)

Bahcall, J.N., Bahcall, N.A. and Weistrop, D. 1975, Ap. J. (Lett.) 16, L159.

Bahcall, J.N. and Ostriker, J.P. 1975, Nature 256, 23.

Bahcall, J.N. and Wolf, R.A. (BW) 1976, Ap. J. 209, 214.

Bahcall, J.N. and Wolf, R.A. 1977, Ap. J. 216, 883.

Bahcall, N.A. 1976, Ap. J. (Lett.), 204, L83.

Bahcall, N.A. and Hausman, M.A. 1976, Ap. J. (Lett.) 207, L181.

Bahcall, N.A., Lasker, B.M and Wamsteker, W. 1977, Ap. J. (Lett.) 213, L105.

Begelman, M.C. and Rees, M.J. 1978, MNRAS 185, 847.

Bisnovatyi-Kogan, G.S., Churayev, R.S. and Kolosov, B.I. 1982, Astron. Astrophys. 113. 179.

Chandrasekhar, S. 1942, Principles of Stellar Dynamics (Chicago: University of Chicago Press).

Cohn, H. 1979, Ap. J. 234, 1036.

Cohn, H. 1980, Ap. J. 242, 765.

Cohn, H. and Hut, P. 1983, preprint.

Cohn, H. and Kulsrud, R.M. 1978, Ap. J. 226, 1087.

Colgate, S.A. 1967, Ap. J. 150, 163.

Djorgovski, S. and King, J.R. 1984, Ap. J. (Lett.) 277, L49.

Dokuchayev, V.I. and Ozernoi, L.M. 1977, JETP 73, 1587.

Duncan, M.J. and Shapiro, S.L. 1982, Ap. J. 253, 921 (Paper IV).

Duncan, M.J. and Shapiro, S.L. 1983, Ap. J. 268, 565.

Einstein, A. 1939, Ann. Math. 40, 922.

Fackerell, E.D., Ipser, J.R. and Thorne, K.S. 1969, Comments Astrophys. Space Phys. 1, 134.

Fall, S.M. and Malkam, M.A. 1978, MNRAS 185, 899.

Farouki, R.T., Shapiro, S.L. and Teukolsky, S.A. 1983, in IEEE Computer 16, 73.

Frank, J. 1978, MNRAS 184, 87.

Frank, J. and Rees, M.J. 1976, MNRAS 176, 633.

Goodman, J. 1983, preprint.

Grindlay, J.E. 1977 in Highlights of Astronomy Vol. 4, 111.

Grindlay, J.E. 1981, in X-ray Astronomy with the Einstein Satellite ed. R. Giacconi (Reidel, Dordrecht) p. 79.

Grindlay, J.E. 1983, Advances in Space Exploration Vol. 2, No. 9, p. 133.

Grindlay, J.E., Hertz, P., Steiner, J.E., Murray, S.S. and Lightman, A.P. 1984, Ap. J. (Lett.) 282, L13.

Gursky, H. and Schwartz, D.A. 1977 in Ann. Rev. Astron. Astrophys. 15, 541.

Heggie, D.C. 1983, preprint.

Hénon, M. 1961, Ann. d'Ap. 24, 369.

Hénon, M. 1975 in Dynamics of Stellar Systems (IAU Symposium No. 69), ed. by A. Hayli (Reidel, Dordrecht) p. 133.

Hills, J.G. 1975, Nature 254, 295.

Inagaki, S. and Lynden-Bell, D. 1983, MNRAS 205, 913.

Ipser, J.R. 1969, Ap. J. 158, 17.
Ipser, J.R. 1978, Ap. J. 222, 976.
Ipser, J.R. 1980, Ap. J. 238, 1101.
Lightman, A.P. 1976, private communication in Bahcall and Wolf (1976).
Lightman, A.P. 1982, Ap. J. (Lett.) 263, L19.
Lightman, A.P., Press, W.H. and Odenwald, S. 1978, Ap. J. 219, 629.
Lightman, A.P. and Shapiro, S.L. (LS) 1977, Ap. J. 211, 244.
Lightman, A.P. and Shapiro, S.L. 1978, Rev. Mod. Phys. 50, 437.
Lin, D.N.C. and Tremaine, S. 1980, Ap. J. 242, 789.
Lynden-Bell, D. 1967, MNRAS 136, 101.
Lynden-Bell, D. 1969, Nature 223, 690.
Lynden-Bell, D. and Eggleton, P.P. 1980, MNRAS 138, 495.
Marchant, A.B. and Shapiro, S.L. 1979, Ap. J. 234, 317 (Paper II).
Marchant, A.B. and Shapiro, S.L. 1980, Ap. J. 239, 685 (Paper III).
McMillan, S.L., Lightman, A.P. and Cohn, H. 1981, Ap. J. 251, 436.
Norman, C. and Silk, J. 1983, Ap. J. 266, 502.
Peebles, P.J.E. 1972a, Gen. Rel. Grav. 3, 63.
Peebles, P.J.E. 1972b, Ap. J. 178, 371.
Rees, M.J. 1977, Ann. N.Y. Acad. Sci. 302, 613.
Rees, M.J. 1978, Phys. Scripta 17, 193.
Rees, M.J. 1984 in Ann. Rev. Astron. Astrophys., in press.
Sanders, R. 1970, Ap. J. 162, 791.
Sargent, W.L.W., Young, P.J., Boksenberg, A., Shortridge, K., Lynds,
    C.R. and Hartwick, F.D.A. 1978, Ap. J. 221, 731.
Shapiro, S.L. 1977, Ap. J. 217, 281.
Shapiro, S.L. and Lightman, A.P. 1976, Nature 262, 743.
Shapiro, S.L. and Marchant, A.B. 1978, Ap. J. 225, 603 (Paper I).
Shapiro, S.L. and Teukolsky, S.A. 1985 (a,b,c) in preparation.
Silk, J. and Arons, J. 1975, Ap. J. (Lett.) 200, L131.
Spitzer, L. 1940, MNRAS 100, 396.
Spitzer, L. 1962, Physics of Fully Ionized Gases (Wiley, New York).
Spitzer, L. 1971 in Semaine d'etude sur les noyeaux des galaxies 1970
    (Pontificae Academiae Scientarum Scripta Varia No. 34).
Spitzer, L. 1975 in Dynamics of Stellar Systems (IAU Symposium No 69),
    ed. by A. Hayli (Reidel, Dordrecht), p. 3.
Spitzer, L. and Hart, M.H. 1971, Ap. J. 164, 399.
Strittmatter, P.A. and Williams, R.E. 1976 in Ann. Rev. Astron.
    Astrophys. 14, 373.
Truran, J.W. and Cameron, A.G.W. 1972, Ap. and Space Sci. 14, 179.
Ulrich, M.H., Boksenberg, A., Bromage, G.E., Clavel, J., Elvius, A.,
    Penston, M.V., Perola, G.C., Petteni, M., Snijders, M.A.J., Tanzi,
    E.G. and Tarenghi, M. 1984, MNRAS 206, 221.
Wielen, R. 1971, Ap. Space Sci. 13, 300.
Wolfe, A.M. and Burbidge, G.R. 1970, Ap. J. 161, 419.
Wyller, A.A. 1970, Ap. J. 160, 443.
Young, P.J., Shields, G.A. and Wheeler, J.C. 1977, Ap. J. 212, 367.
Young, P.J., Westphal, J.A., Kristian, J., Wilson, C.P. and Landauer,
    F.P. 1978, Ap. J. 221, 721.
Zel'dovich, Ya. B. and Novikov, I.D. 1971, Relativistic Astrophysics,
    Vol. 1 (University of Chicago, Chicago).

Zel'dovich, Ya. B. and Podurets, M.A. 1965, Astron. Zh 42, 963 [English translation in Sov. Astron. - A.J. 9, 742].

DISCUSSION

KING: Another version of Peebles' remark (not due to Peebles) is, "I'll believe a black hole when I see one." More seriously, what would you expect us to observe, that would distinguish between your model and those that are stabilized by binaries?

SHAPIRO: As has been pointed out for a long time, black holes will induce distinguishing 'cusp' profiles in the cores of any cluster in which they reside. These central cusps will take a number of forms: optical light cusps, star-count surface density cusps (σ), and projected rms velocity cusps, $V_\parallel$ (averaged through the line of sight). Of these, the most frequently mentioned is σ, which acquires the characteristic Bahcall-Wolf $\sigma \sim r^{-3/4}$ shape. It will be difficult, however, to distinguish this profile observationally from asymptotic isothermal profiles, $\sigma_{isoth} \sim r^{-1}$, which may characterize post-collapse binary scenarios. However, as Marchant and I emphasized in Paper III of our series (see, e.g. Fig. 12), $V_\parallel$ may provide the *best* evidence for the presence of a massive, central black hole. This function rises rapidly ad $V_\parallel \sim r^{-1/2}$ inside the core, while, as Cohn has pointed out, it does not increase very rapidly in clusters without massive holes.

One should also pursue *statistical* studies of cumulative cluster data to distinguish between the different post-collapse evolutionary tracks that clusters follow, depending on whether they contain a massive black hole or binaries. One might ultimately produce 'H-R' diagrams in which the location of clusters reveals pre- and post-collapse evolutionary paths. This may be difficult, of course, particularly since at late times the post-collapse core expansion may be quite comparable in both scenarios. Nevertheless, this study should be pursued further.

COHN: As a follow-up the previous question, I would like to note that the behavior of the velocity dispersion profile in a cusp should give the best indication of whether a massive central black hole is present. In a cusp around a black hole, $\nu \propto r^{-0.5}$ and is thus fairly steep. In contrast, in a cusp that developes as a result of core collapse with no black hole, the velocity dispersion is very much flatter, $\nu \propto r^{-0.11}$.